ROBUST MULTI-OBJECTIVE OPTIMISATION OF A DESCENT GUIDANCE STRATEGY FOR A TSTO SPACEPLANE

Lorenzo A. Ricciardi[a], Christie Alisa Maddock[a], Massimiliano Vasile[a], Tristan Stindt[b], Jim Merrifield[b]
Marco Fossati[a], Michael West[c], Konstantinos Kontis[d], Bernard Farkin[e], Stuart McIntyre[e]

[a]University of Strathclyde, Glasgow, UK
[b]Fluid Gravity Engineering, Emsworth, UK
[c]BAE Systems, Prestwick, UK
[d]University of Glasgow, Glasgow, UK
[e]Orbital Access, Prestwick, UK

ABSTRACT

This paper presents a novel method for multi-objective optimisation under uncertainty developed to study a range of mission trade-offs, and the impact of uncertainties on the evaluation of launch system mission designs. A memetic multi-objective optimisation algorithm, MODHOC, which combines the Direct Finite Elements transcription method with Multi Agent Collaborative Search, is extended to account for model uncertainties. An Unscented Transformation is used to capture the first two statistical moments of the quantities of interest. A quantification model of the uncertainty was developed for the atmospheric model parameters. An optimisation under uncertainty was run for the design of descent trajectories for the Orbital-500R, a commercial semi-reusable, two-stage launch system under development by Orbital Access Ltd.

Index Terms— Spaceplane, Optimisation under Uncertainty,

1. INTRODUCTION

This paper presents a novel method for multi-objective optimisation under uncertainty, developed to study a range of mission trade-offs and the impact of uncertainties on system models for launch systems. This is applied to the analysis and design of descent trajectories for the Orbital-500R, a commercial semi-reusable, two-stage launch system under development by Orbital Access.

The set of Pareto-optimal solutions show the trade-off between minimising the induced acceleration limits and maximising the robustness of the solutions by minimising the sensitivity to uncertainties.

Uncertainty quantification (UQ), the science of quantifying the uncertainty in the desired performance of a system, can be a key step in analysing the robustness of a control solution and of the whole guidance, navigation and control (GNC) chain. Common approaches to UQ use extensive Monte Carlo simulations to account for errors, unmodelled components and disturbances. At system level, UQ analysis can translate into the assessment of the whole system reliability or the reliability of one or more components. An uncertainty quantification analysis is, therefore, a fundamental step towards de-risking any technological solution as it provides a quantification of the variation in performance and probability of recoverable or unrecoverable system failures, given existing information.

Within the current preliminary design phase of the Orbital-500R, one of the areas of study is the uncertainty related to the aerodynamic modelling of the re-usable spaceplane.

The goal is, therefore, to design a robust guidance trajectory considering the uncertainty related to the atmospheric model which in turn affects the aero-, aerothermal and flight dynamics. Furthermore, given the early stage of the vehicle design and the wide scope of use required by the commercial side, a number of re-entry scenarios are possible, each of which is affected differently by the same sets of uncertainties.

This paper presents an extension of the capabilities of MODHOC to account for uncertainties. The extension is based on an Unscented Transformation to capture the first two statistical moments of the quantities of interest. The result is an unscented multi-objective optimal control approach that can efficiently handle the level of uncertainty in model parameters. Using multiple objective functions, trade-off studies on the Orbital-500R design will be presented for the chosen performance and vehicle characteristics of the re-entry trajectory and the robustness of those performances (and the associated guidance laws) against the uncertainty of the atmospheric model.

2. OPTIMAL CONTROL

Multi-Objective Direct Hybrid Optimal Control (MODHOC) [1, 2] is based on Direct Finite Elements Transcription

(DFET), a transcription method for nonlinear multi-phase optimal control problems [3], with MACS, a population based memetic multi-objective optimisation algorithm [4] and mathematical programming solvers. The DFET transcription method allows to treat general optimal control problems, thus it can tackle problems with any kind of dynamic model. The memetic multi-objective optimisation algorithm MACS allows for a global exploration of the search space and is able to treat problems with an arbitrary number of objectives. The mathematical programming solvers are used to refine the solutions obtained and guarantee the local optimality of the solutions found while also satisfying tight constraints.

The software has been successfully used for the trajectory and design optimisation of vertical and horizontal launch systems [5, 6], deployment of constellations [7], interplanetary exploration missions [8] and the design of multi-debris removal missions.

2.1. Unscented optimal control

In order to perform robust optimisation of the re-entry trajectory of the Orbital 500R, an Unscented Transformation [9] was included in the formulation of the optimal control problem.

Unscented Transformations capture the first statistical moments, mean and covariance, of the distributions of the states of a system subject to uncertainty and undergoing arbitrary non-linear transformations by propagating a small number of sigma points. If the system depends on N_{uq} uncertain variables, whose mean and covariances are known, the unscented transformation requires the propagation of $2N_{uq}+1$ samples. The first sigma point takes the mean value for all the uncertain variables, while the others assume the mean plus (or minus) the square root of the matrix of the covariances of the uncertain variables. All the sigma points are propagated simultaneously with the mean and covariance of the final states computed as a weighted combination of the final states of each sigma point.

The approach employed in this paper follows the one described by [10]. Let the dynamics of the systems be given by

$$\dot{\mathbf{x}} = \mathbf{F}(\mathbf{x}, \mathbf{u}, \mathbf{b_{uq}}, t) \tag{1}$$

where $\mathbf{x}$ are the states of the system, $\mathbf{u}$ are the controls, t is time, and b_{uq} are additional static parameters which are here assumed to be affected by uncertainty. The dynamics of each sigma point $\boldsymbol{\chi}_i, i = 1\ldots, 2N_{uq}+1$ is given by $\dot{\boldsymbol{\chi}}_i = \mathbf{F}(\boldsymbol{\chi}_i, \mathbf{u}, \mathbf{b}_i, t)$.

This means that each sigma point has a different value for the static variables, its dynamics evolve independently of the other sigma points, but all sigma points are controlled by the same control law. The idea is thus to find a single control law that, when applied to all sigma points, allows the ensemble to reach a desired final condition and to be optimal in some sense. The particular values for each static variable $\mathbf{b}_i$ is decided by the application of the Unscented Transformation.

A known problem of the Unscented Transformation is that it can generate covariance matrices that are not semidefinite positive. To avoid this problem, a more recent and stable version of the Uncertain Transformation was employed in this paper, called the Square Root Unscented Transformation [11]. Algorithmically it is very similar to the standard version, but it differs in the way the samples are generated and has the advantage that the resulting covariance matrix is guaranteed to be semidefinite positive (up to machine precision). In practice, the sigma points are thus computed from the Cholesky factorisation of the covariance matrix, and slightly different algebraic manipulations are performed to obtain the covariance matrix of the transformed states.

Mathematically, thus, the problem can be described as follows: let $\boldsymbol{X}$ be a state vector of length $N_\sigma N_x$,

$$\mathbf{X} := \left[\boldsymbol{\chi}^0, \boldsymbol{\chi}^1, \cdots, \boldsymbol{\chi}^{N_\sigma}\right]^T \tag{2}$$

where N_σ is the number of sigma points and N_x is the number of states of the original system. The dynamics of this system is then given by

$$\dot{\mathbf{X}} := \begin{bmatrix} \mathbf{f}(\boldsymbol{\chi}^{\mathbf{0}}, \mathbf{u}, \boldsymbol{b}_0, t) \\ \mathbf{f}(\boldsymbol{\chi}^{\mathbf{1}}, \mathbf{u}, \boldsymbol{b}_1, t) \\ \vdots \\ \mathbf{f}(\boldsymbol{\chi}^{\mathbf{N}_\sigma}, \mathbf{u}, \boldsymbol{b}_{N_\sigma}, t) \end{bmatrix} := \mathbf{F}(\mathbf{X}, \mathbf{u}, \mathbf{B}, t) \tag{3}$$

The multi-objective unscented optimal control problem can thus be formulated as

$$\begin{aligned} &\min_{\mathbf{u}\in U} \mathbf{J}(\mathbf{X}, \mathbf{u}, \mathbf{B}, t) \\ &s.t. \\ &\dot{\mathbf{X}} = \mathbf{F}(\mathbf{X}, \mathbf{u}, \mathbf{B}, t) \\ &\mathbf{g}(\mathbf{X}, \mathbf{u}, \mathbf{B}, t, \geq 0 \\ &\boldsymbol{\psi}(\mathbf{X}(t_0), \mathbf{X}(t_f), \mathbf{u}(t_0), \mathbf{u}(t_f), \mathbf{B}, t_0, t_f) \geq 0 \\ &t \in [t_0, t_f] \end{aligned} \tag{4}$$

In this work, since there is no uncertainty about the initial state of the system, the initial conditions are expressed as usual. The final conditions, instead, are expressed as difference between the mean and the target value.

$$\boldsymbol{\psi}(\mathbf{X}(t_f)) := \boldsymbol{\mu}_\chi - \overline{x}(t_f) = 0 \tag{5}$$

where $\boldsymbol{\mu}_\chi$ is the mean of the final states of the sigma points, and $\overline{x}(t_f)$ is the target value. The first objective

$$J_1 := \int_{t_0}^{t_f} E(\mathbf{a}^2) dt \tag{6}$$

is the integral of the expected value of the square of the total accelerations $\mathbf{a}$, which should guarantee that the accelerations will be minimised on average along all the trajectory.

The second objective is meant to reduce the uncertainty of the final state. To this end, the sum of the square of all the entries of the covariance matrix of the final states is minimised.

$$J_2 = \sum_{i,j} \left(\mathrm{Cov}_{i,j}(\mathbf{X}(t_f)\right)^2 \tag{7}$$

where $\mathrm{Cov}_{i,j}$ is computed using the standard algebraic manipulations employed for the Square Root Unscented transformation, with the additional consideration that no update of the Cholesky factorisation is needed since no measurement is here performed and thus no error is present. This formulation has the advantage that the quantity to compute is smooth and differentiable, it involves all components of the covariance matrix, and does not require iterative procedures like decomposition in eigenvalues to compute the principal axes of the ellipsoid of the uncertainty. In order to give each element of the covariance matrix the same weight even if the quantities of interest have different scales, the state variables were scaled by the same factors internally employed by MODHOC to ensure that all variables assume values between 0 and 1.

3. VEHICLE SYSTEM MODELS

The Orbital-500R system is composed of a first stage reusable spaceplane, capable of rocket-powered ascent and an unpowered, glided descent, and an expendable, rocket-based upper stage. The dry mass of the spaceplane is 20 tonnes.

The flight dynamics are modelled as a variable-mass point with three degrees of freedom in the Earth-centered Earth-fixed reference frame, subject to gravitational, aerodynamic lift and drag forces. The state vector contains the translational position and velocity, and time-dependant vehicle mass, $\mathbf{x} = [h,\, \lambda,\, \theta,\, v,\, \gamma,\, \chi, m]$ where h is the altitude, (λ, θ) are the geodetic latitude and longitude, v is the magnitude of the relative velocity vector directed by the flight path angle γ and the flight heading angle χ [12]. The vehicle is controlled through the angle of attack α, and the bank angle μ of the vehicle. The Earth is modelled as a perfect sphere of radius R_E.

The aerodynamic coefficients were modelled using an artificial neural network with given an aerodynamic database for the training data coming from CFD simulations [13].

From previous work on the optimisation of the full ascent and reentry trajectory, the vehicle is assumed to begin its reentry (at time $t = 0$) with the following initial conditions:

$$\begin{aligned}
\text{Altitude } h(0) &= 90\,\mathrm{km} \\
\text{Latitude } \lambda(0) &= 60^\circ N \\
\text{Longitude } \theta(0) &= -12^\circ E \\
\text{Velocity } v(0) &= 3\ \text{km/s} \\
\text{Flight path angle } \gamma(0) &= -5^\circ \\
\text{Heading angle } \chi(0) &= 20^\circ
\end{aligned}$$

The only final condition imposed was the expected value of the altitude, with a value of $10\,\mathrm{km}$. In addition, the trajectories of all sigma points were required to have a flight path angle greater or equal to -20°.

4. UNCERTAINTY QUANTIFICATION

Analysis to date on the design of the Orbital 500-R has employed the US-76 Standard atmospheric model [14]. The US-76 is a global static standard model, giving the atmospheric pressure p, temperature T and density ρ as function of altitude up to 1000 km.

In order to assess the robustness of the design against uncertainties in the atmospheric model, it was necessary to develop a model for its uncertainty. To this end the NRLMSISE-00 [15] atmospheric model was employed. It is more recent and sophisticated than the US76 model, and takes into account several factors like daily and seasonal effects, solar and magnetic activity and geographical dependencies. This model thus gives temperature and density as a function of 7 other input parameters in addition to altitude.

A statistical analysis of the difference of the models was performed treating those 7 additional input parameters as uncertain. 100000 samples were taken from the low discrepancy Halton sequence, and the corresponding values for T and ρ were computed using the NRLMSISE-00 model for all altitudes in the range between 0 and 100 km.

To account for the possible differences between the models, the relative average difference between the values of the two model was computed for all the thermodynamic quantities. These relative errors were then treated as random fluctuations, for which averages and covariances were computed as a function of altitude. These relative errors and covariances deviations are plotted in Figures 1, 2 and 3.

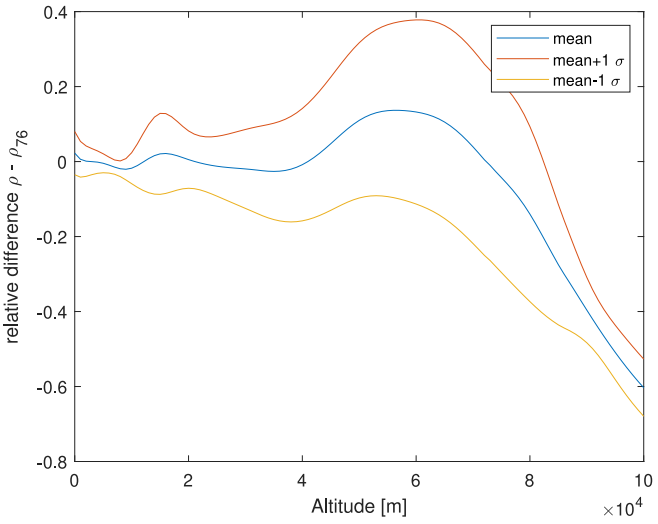

Fig. 1. Relative error between models, density

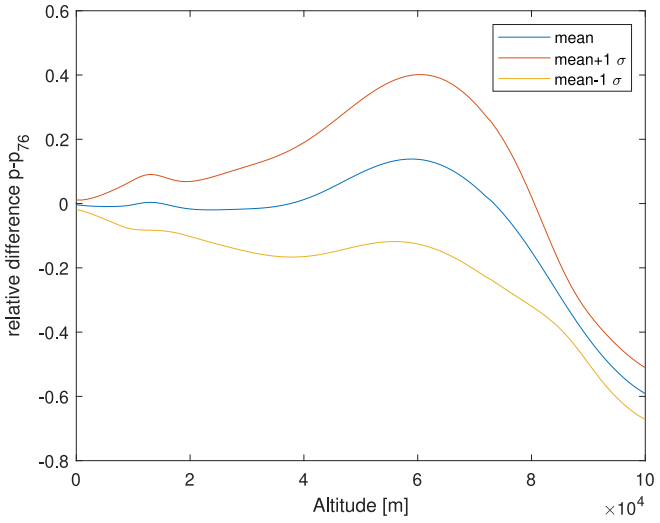

Fig. 2. Relative error between models, pressure

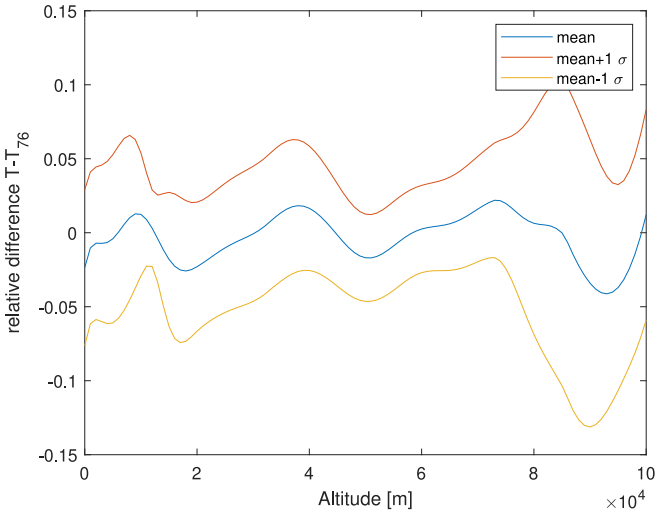

Fig. 3. Relative error between models, temperature

It can be observed that for the temperature the mean relative errors are very low, with a 1σ relative error around 5% for altitudes below 80 km. The mean relative errors for pressure and density are also low for relatively low altitudes, but they tend to drift systematically at higher altitudes, and the 1σ bands are much wider. This happens above 40km where pressure and density have a very low absolute value, so a large relative error still means a low absolute error. It is thus expected that the impact of these relatively high differences in density between the two models will not affect significantly the first part of the trajectory.

Since the approach employed is that of the Square Root Unscented Transformation, different models were generated: one employing the mean relative error, and the others adding to the mean the Cholesky factorisation of the covariance matrix of the uncertain quantities at each altitude. Figure 4 shows the five generated temperature profiles, and their comparison with respect to the US76 model. A similar approach was followed for the density. As it can be seen, the model referred to as Sigma point 0 is quite close to the US76 model. Sigma ponts 1 and 2 add the standard deviation to this mean, while Sigma ponts 3 and 4 also include the correlation between variations in temperature and variations in density. The correlation between temperature and density changes sign repeatedly as the altitude changes, thus the profiles assume values lower than one standard deviation only to cross the mean and assume values higher than one standard deviation elsewhere. Among the 100000 samples generated by the Halton sequence on the NRLMSISE-00 model, several profiles do indeed have this kind of shape, which is significantly different to the US76 model. The temperature affects the computation of the Mach number, on which the aerodynamic coefficients depend. The dependence of the aerodynamic coefficients on the Mach number is stronger around Mach 1 and weaker for high Mach numbers, thus it is not easy to foresee the effect of these variations. Including these sigma points in the design of a robust guidance law is thus expected to make it more robust.

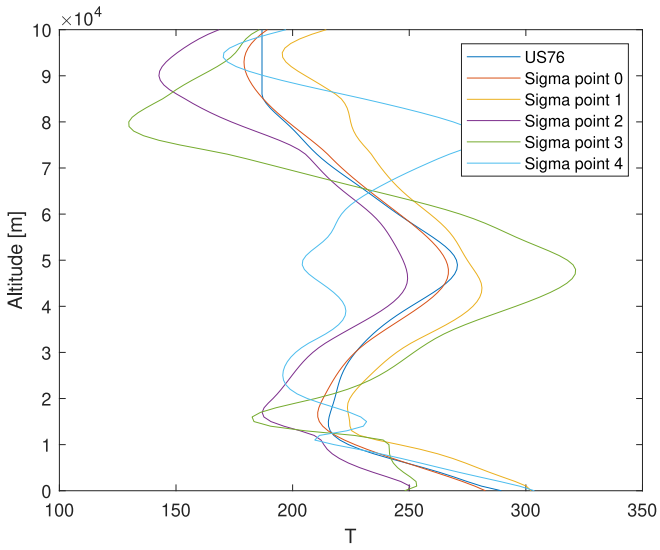

Fig. 4. Temperature profiles for the models of each sigma point, and comparison with the US76 model

5. RESULTS

The equations were discretised employing the DFET transcription included in MODHOC, using 3 elements of order 7 for all the states and the controls. Since all the sigma points are propagated simultaneously, this means that there are 30 states and 2 controls, making it a rather large problem. In order to have a good approximation of the Pareto Front, MODHOC was run for a total of 30000 function evaluations, keep-

ing 10 solutions in the archive. The computed Pareto front is shown in Fig. 5, which confirms a trade-off between the expected total acceleration load and the total uncertainty of the final state.

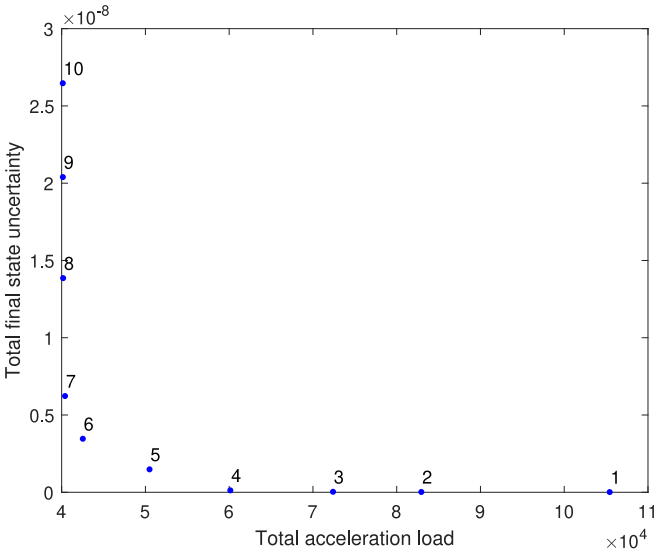

Fig. 5. Pareto Front

Figure 6 show the time histories of the altitude for all the solutions in the archive, 7 shows the flight path angle and 8 the velocity, with the dashed and dotted lines indicating the 1σ uncertainty.

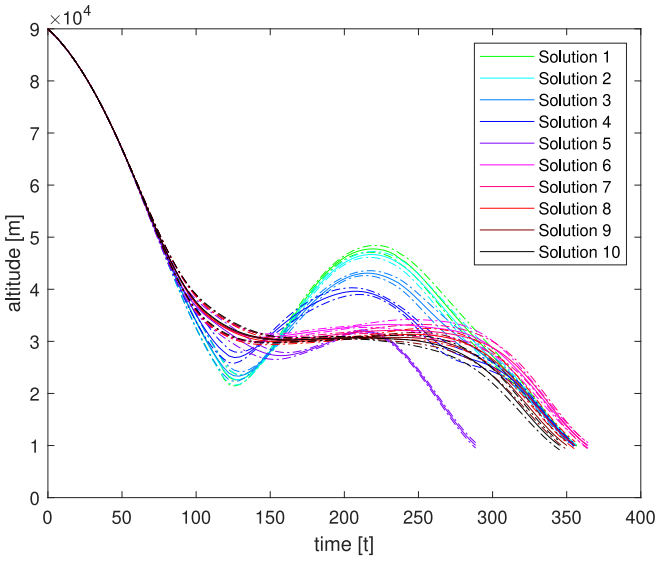

Fig. 6. Altitude vs time

In all these plots it is possible to see that solutions in green, light blue and blue (Solutions 1 to 4) have lower uncertainty for the final state. This can also be seen from Figures 9, 10 and 11, which show the standard deviation of altitude,

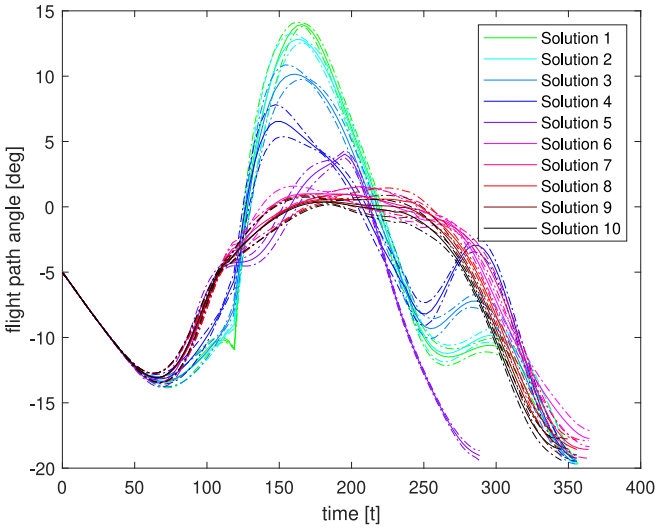

Fig. 7. Flight path angle vs time

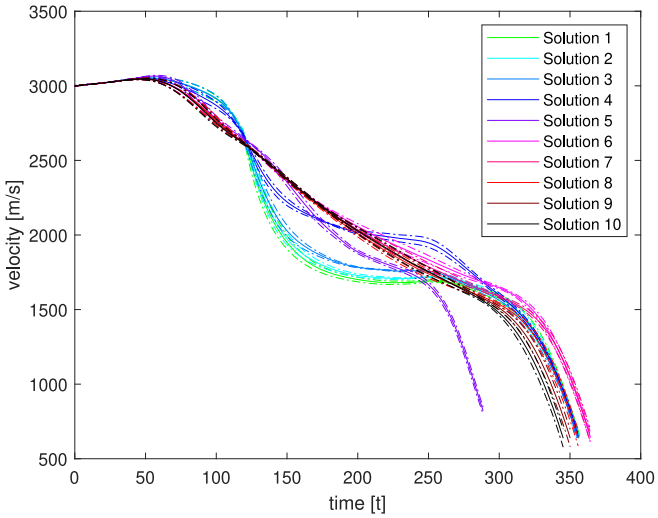

Fig. 8. Velocity vs time

flight path and velocity as a function of time. As previously stated, even if the uncertainty on density is relatively high at high altitudes, its effect is quite limited for the first part of the trajectory. However, it becomes more important as the altitudes get to approximately $40\,\mathrm{km}$.

This as the Pareto front was showing, solutions associated with lower uncertainty in final states have higher acceleration loads, as shown in 12.

Figure 13 shows the time history for the control α. In all cases, the angle of attack starts with the maximum possible value of $45\,\mathrm{deg}$, and then progressively decreases to a more moderate value around $5 - 10\,\mathrm{deg}$. Solutions with lower accelerations stay in this regime for a while, and finally conclude with a value around $0\,\mathrm{deg}$. Solutions with lower final uncertainty instead have a progressive decrease in α until

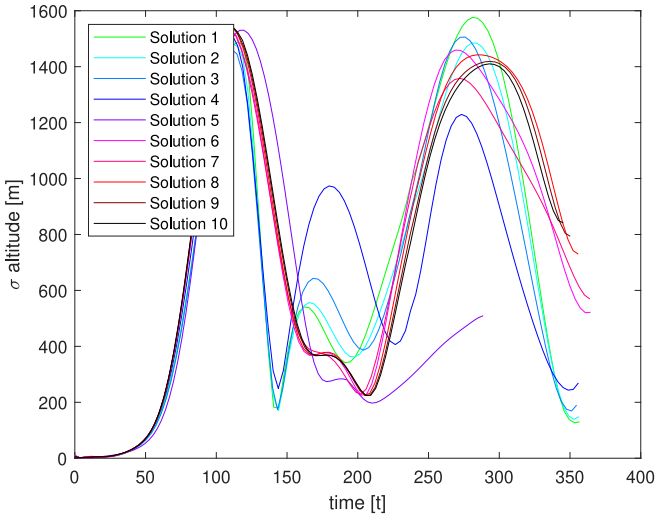

Fig. 9. Altitude vs time, standard deviations

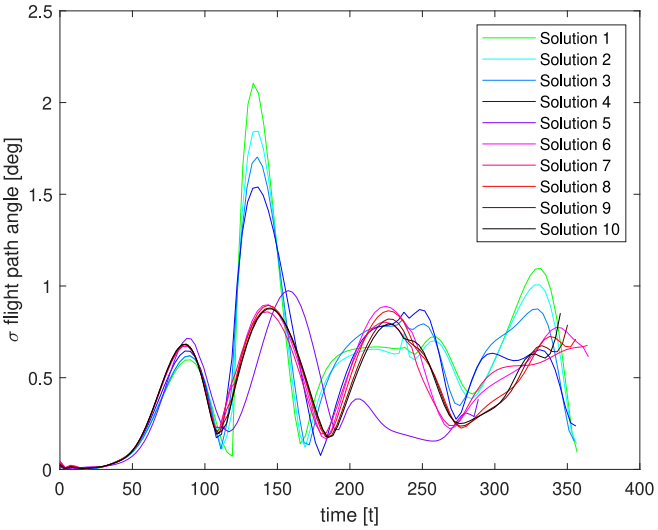

Fig. 10. Flight path angle vs time, standard deviations

small negative values, then a sharp increase to values around $10 - 15\,\mathrm{deg}$, and finally stabilise around $0\,\mathrm{deg}$ like the other trajectories.

Finally, Figures 14, 15 and 16 show the time history of altitude, flight path angle and velocity of all sigma points for Solution 1 and 10. As it is evident, the green lines have a much lower scattering at the final time than the black lines, indicating that Solution 1 (green) is subject to less uncertainty than solution 10 (black). This figures also give an idea of the complexity of the problem tackled by this approach, where the same control law is applied to multiple independent sigma points (lines with the same colour) and is able to steer the system to a given expected final state while also reducing the uncertainty associated to the final state, or reducing the expected acceleration load.

6. CONCLUSIONS

This paper presented and extension of MODHOC to perform robust multi-objective optimisation of the reentry trajectories of the Orbital 500R. Employing the Unscented Transformation, a different atmospheric model was developed for each of the sigma points. All the sigma points share the same control law, thus making the trajectory robust against model uncertainty. Albeit only the first two statistical moments of the uncertain values were considered for this work, it is possible to account for higher order moments, making the resulting trajectory even more robust. To this end, however, a larger number of sigma points will be required, and the resulting optimal control problem becomes progressively larger, requiring the use of large scale optimisation code.

7. ACKNOWLEDGEMENTS

This work has been partially funded by the UK Space Agency and European Space Agency (ESA) General Support Technology Programme (GSTP).

8. REFERENCES

[1] Lorenzo A Ricciardi, Massimiliano Vasile, and Christie Maddock, "Global solution of multi-objective optimal control problems with multi agent collaborative search and direct finite elements transcription," in *2016 IEEE Congress on Evolutionary Computation (CEC)*. IEEE, 2016, pp. 869–876.

[2] Lorenzo A. Ricciardi, Christie A. Maddock, and Massimiliano Vasile, "Direct solution of multi-objective optimal control problems applied to spaceplane mission design," *Journal of Guidance, Control and Dynamics*, 2018.

[3] Massimiliano Vasile, "Finite elements in time: A direct transcription method for optimal control problems," in *AIAA/AAS Astrodynamics Specialist Conference, Guidance, Navigation, and Control and Co-located Conferences*, Toronto, Canada, 2-5 Aug 2010.

[4] Lorenzo A. Ricciardi and Massimiliano Vasile, "Improved archiving and search strategies for multi agent collaborative search," in *International Conference on Evolutionary and Deterministic Methods for Design, Optimization and Control with Applications to Industrial and Societal Problems (EUROGEN)*, Glasgow, UK, 14-16 Sep 2015.

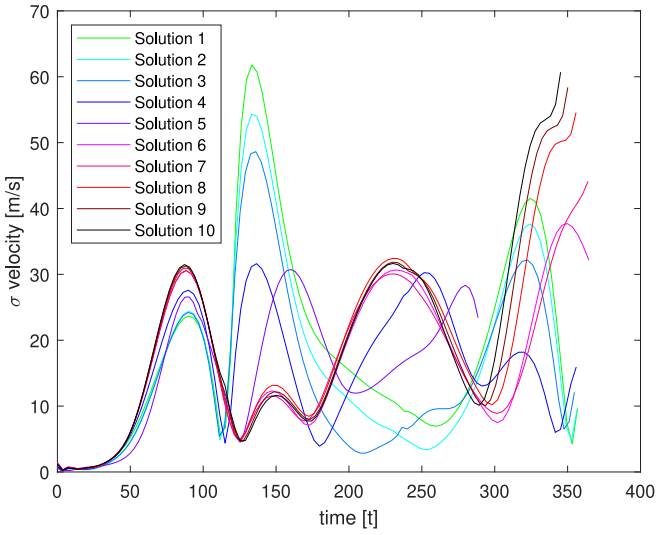

Fig. 11. Velocity vs time, standard deviations

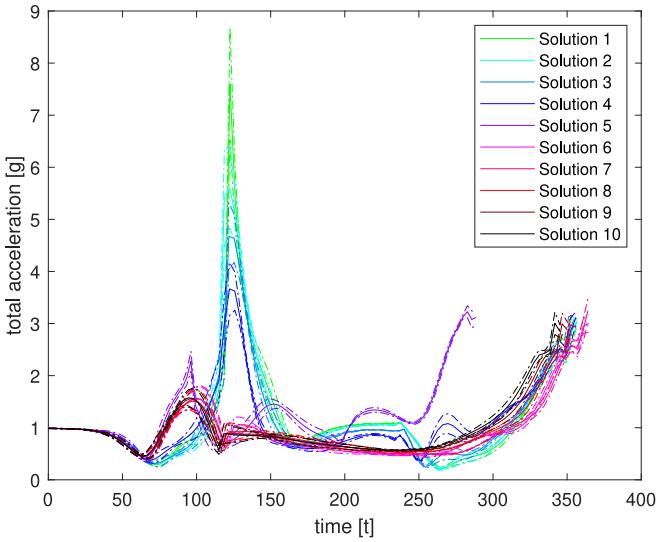

Fig. 12. Total acceleration vs time

[5] Lorenzo Angelo Ricciardi, Massimiliano Vasile, Federico Toso, and Christie A Maddock, "Multi-objective optimal control of the ascent trajectories of launch vehicles," in *AIAA/AAS Astrodynamics Specialist Conference*, 2016, p. 5669.

[6] Massimiliano L Vasile, Christie Maddock, and Lorenzo Ricciardi, "Multi-objective optimal control of re-entry and abort scenarios," in *2018 Space Flight Mechanics Meeting*, 2018, p. 0218.

[7] Marilena Di Carlo, Lorenzo Ricciardi, and Massimiliano Vasile, "Multi-objective optimisation of constellation deployment using low-thrust propulsion," in *AIAA/AAS Astrodynamics Specialist Conference*, 2016, p. 5577.

[8] Federico Zuiani, Yasuhiro Kawakatsu, and Massimiliano Vasile, "Multi-objective optimisation of many-revolution, low-thrust orbit raising for destiny mission," in *23rd AAS/AIAA Space Flight Mechanics Conference*, Kauai, Hawaii, 10-14 Feb 2013.

[9] Simon J Julier and Jeffrey K Uhlmann, "A general method for approximating nonlinear transformations of probability distributions," Tech. Rep., Robotics Research Group, Department of Engineering Science, University of Oxford, 1996.

[10] I Michael Ross, Ronald J Proulx, Mark Karpenko, and Qi Gong, "Riemann–Stieltjes optimal control problems for uncertain dynamic systems," *Journal of Guidance, Control, and Dynamics*, vol. 38, no. 7, pp. 1251–1263, 2015.

[11] R. Van der Merwe and E. A. Wan, "The square-root unscented Kalman filter for state and parameter-estimation," in *2001 IEEE International Conference on Acoustics, Speech, and Signal Processing Proceedings (Cat. No.01CH37221)*. IEEE.

[12] Peter Zipfel, *Modeling and Simulation of Aerospace Vehicle Dynamics, Second Edition*, AIAA Education Series, 2007.

[13] Christie Alisa Maddock, Lorenzo Ricciardi, Michael West, Joanne West, Konstantinos Kontis, Sriram Rengarajan, David Evans, Andy Milne, and Stuart McIntyre, "Conceptual design analysis for a two-stage-to-orbit semi-reusable launch system for small satellites," *Acta Astronautica*, vol. 152, pp. 782–792, 2018.

[14] NASA NOAA and US Air Force, "US Standard Atmospheres," *Washington, DC: US Government Printing Office*, pp. 53–63, 1976.

[15] J. M. Picone, A. E. Hedin, D. P. Drob, and A. C. Aikin, "NRLMSISE-00 empirical model of the atmosphere: Statistical comparisons and scientific issues," *Journal of Geophysical Research: Space Physics*, vol. 107, no. A12, 2002.

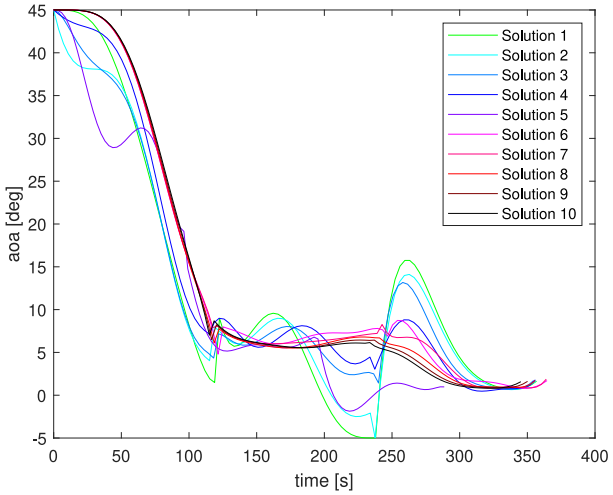

Fig. 13. Angle of attack vs time

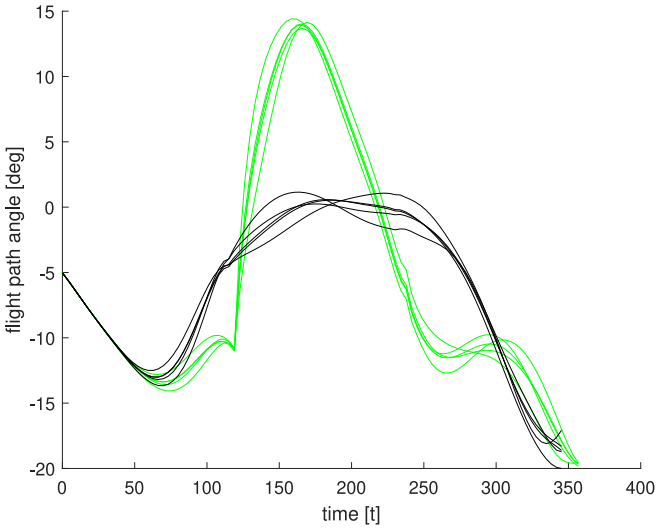

Fig. 15. Time history of the flight path angle for all sigma points of Solutions 1 and 10

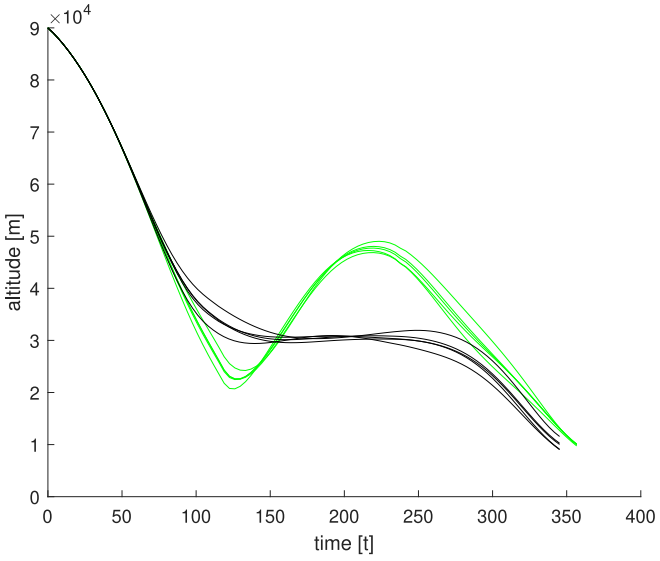

Fig. 14. Time history of the altitude for all sigma points of Solutions 1 and 10

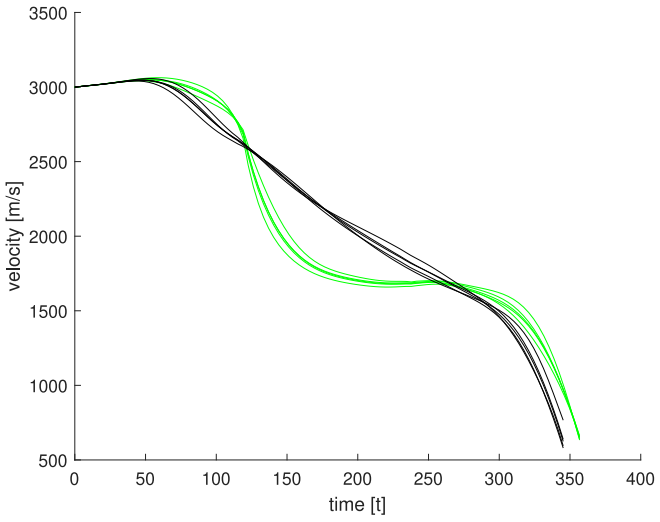

Fig. 16. Time history of the velocity for all sigma points of Solutions 1 and 10